Ratcheting of neutral elastic dimers on a charged filament

Andrey Pototsky,[1] Fabio Marchesoni,[2,1] and Sergey E. Savel'ev[1]
[1]*Department of Physics, Loughborough University, Loughborough LE11 3TU, United Kingdom*
[2]*Dipartimento di Fisica, Università di Camerino, I-62032 Camerino, Italy*
(Received 21 December 2009; published 16 March 2010)

We consider an elastic neutral dimer formed by two bound equal masses carrying opposite charges and moving along an electrically active filament in one dimension. An ac electrical field drives the two dimer heads, when set free or bound together to form a rigid rod, to opposite directions, thus yielding a zero net dimer current for zero and infinite elastic constants. Under the same driving conditions, an elastically deformable dimer can get rectified and the ensuing net current maximized for an optimal value of dimer elastic constant. The dependence of the dimer current on the periodic charge distribution along the filament is analyzed in terms of global symmetries of the dimer dynamics.

DOI: 10.1103/PhysRevE.81.031114 PACS number(s): 05.40.−a, 05.60.−k, 68.43.Mn

I. INTRODUCTION

Diffusion and directed transport of charged dimers deposited on a chemically prepared substrate has been extensively studied from a theoretical viewpoint [1–13]. Driven by a time periodic field, $E(t)$, with angular frequency ω, the dimer is rectified in a direction that depends on ω as well as on the asymmetry of the substrate potential. The most intriguing scenario occurs in the case of a neutral dimer consisting of two equal masses with opposite electric charges, $\pm Q$, so that the total driving force is zero [14]. If the dimer is elastically deformable, its internal dynamics causes a nonlinear coupling between the dimer interaction with the substrate and the dimer interaction with the external field, which results in a nonzero net dimer current.

The mechanism of rectification of a neutral dimer is essentially different from that of a single charged ad-dimer, rigid [1,5] or elastic [3,8–10], alike. Indeed, the rectification current of a neutral dimer, if not ruled out by symmetry, is proportional to ω, at low frequencies, and vanishes for $\omega \to \infty$ [14]. This shows that neutral dimer rectification is a strictly nonequilibrium effect. On the contrary, the ratchet current of charged adatoms or ad-dimers is maximum at zero frequency [15], thus allowing for an adiabatic modeling [16,17].

The interaction between a charged adatom and its substrate has generally a complex chemical origin and is commonly assumed to be little affected by the adatom charge [7]. As a consequence, the interaction between the substrate and both heads of a dimer, viewed as two bound adatoms, has also been modeled in terms of a unique substrate potential. In other words, in all models proposed so far, the difference in the coupling between the substrate and the oppositely charged dimer heads was neglected (an exception is discussed in Refs. [12,13]). This is certainly not the case if the substrate is electrically charged.

In this paper, we explicitly address the electrostatic nature of the interaction between an electrically neutral dimer and a charged substrate. To this end, we assume that a diffusive dimer moves along an electrically active filament with L-periodic electrostatic potential $U(x)$, i.e., $U(x+L)=U(x)$, as sketched in Fig. 1. The instantaneous force acting on the positive charge $+Q$, with coordinate x, is given by $F_1=-Q[\partial U(x)/\partial x]$, whereas the force experienced by the negative charge, with coordinate y, is $F_2=Q[\partial U(y)/\partial y]$. Note that models of this type can be specialized to study the functional properties of two-head molecular motors, like kinesin [8,9,18].

The contents of this paper is organized as follows. In Sec. II, we provide the details of our one-dimensional ratchet model for neutral elastic dimers. In Sec. III, we show how a nonzero dimer current only sets on for finite dimer elastic constants. In Sec. IV, we determine the global dynamical symmetries of our model that forbid dimer rectification even in the presence of an asymmetric substrate. In Sec. V, we explain analytically and demonstrate numerically the role of global symmetries in suppressing the dimer current. In Sec. VI, we summarize our results.

II. NEUTRAL DIMER MODEL

The overdamped dynamics of the dimer heads is governed by two coupled Langevin equations

$$\dot{x} = -W'(|x-y|) + F(t) - QU'(x) + \sqrt{2T}\xi_x(t),$$

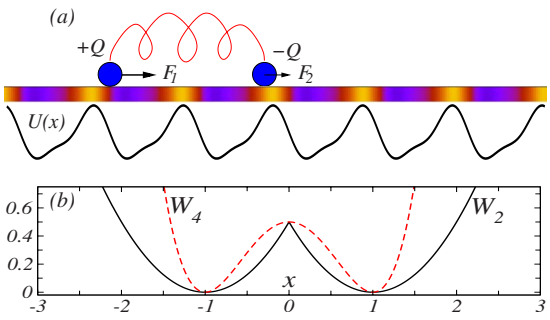

FIG. 1. (Color online) Neutral dimer moving on an electrically active filament. (a) The dimer is formed by two equal masses with coordinates x (left head) and y (right head) carrying opposite charges $\pm Q$. The force exerted by the filament on the two charges are respectively, $F_1=-QU'(x)$ and $F_2=QU'(y)$ (see text) (b) Sketch of the binding potentials W_2, Eq. (2), and W_4, Eq. (3), for $d=\alpha=1$.

$$\dot{y} = + W'(|x-y|) - F(t) + QU'(y) + \sqrt{2T}\xi_y(t), \qquad (1)$$

where $W(|x-y|)$ is the dimer binding potential, $\pm F(t)$, with $F(t)=QE(t)$, are oscillating electrostatic forces, with amplitude QE and angular frequency ω, acting on the dimer heads, T is the dimensionless substrate temperature, and $\xi_i(t)$, with $i=x,y$, are independent zero-mean, Gaussian white noises with autocorrelation functions $\langle \xi_i(t)\xi_j(t')\rangle = \delta_{ij}\delta(t-t')$. Here and in the following, overdots stay for time derivatives and prime symbols denote derivative with respect to whatever argument of the function.

Following Ref. [14], we assume that the elastic properties of the dimer are quantified by the rest length, d, and the elastic constant, α, of two different binding potentials,

(a) the piecewise quadratic bistable potential

$$W_2(|x-y|) = \alpha(|x-y|-d)^2/2, \qquad (2)$$

(b) and the quartic bistable potential

$$W_4(|x-y|) = \alpha(|x-y|^2-d^2)^2/2d^2. \qquad (3)$$

Introducing the new variables $\mu=(x+y)/2$ and $\eta=(x-y)/2$, with μ being the coordinate of the center of mass and η the instantaneous half-length of the dimer, the Langevin equations (1) can be reformulated as

$$\dot{\mu} = -\frac{1}{2}\frac{\partial U_{\rm eff}(\mu,\eta)}{\partial \mu} + \sqrt{T}\xi_\mu(t),$$

$$\dot{\eta} = -\frac{1}{2}\frac{\partial U_{\rm eff}(\mu,\eta)}{\partial \eta} + F(t) + \sqrt{T}\xi_\eta(t), \qquad (4)$$

where $U_{\rm eff}(\mu,\eta)$ is the two-dimensional effective potential

$$U_{\rm eff}(\mu,\eta) = U(\mu+\eta) - U(\mu-\eta) + W(|2\eta|). \qquad (5)$$

Here the stochastic forces $\xi_\mu(t)$ and $\xi_\mu(t)$ have the same statistics as ξ_x and ξ_y, but half their strength, $T/2$ (effective temperature of the new variables).

We emphasize that the η coordinate is related to the time-dependent dipole moment, $2Q\eta$. In two or three dimensions, due to spatial rotations, the projection of the instantaneous dimer polarization on a given axis may change sign. To mimic this effect in one dimension, we allow for η to assume both positive and negative values, by letting the dimer heads pass through one another. The binding potential $W(|2\eta|)$ hinders such a "rotation" mechanism: this is an important difference with respect to the two and three dimensional models cited in Sec. I.

From Eqs. (4) and (5), it is clear that $F(t)=QE(t)$ only couples to the internal degree of freedom of the dimer, represented by η. So, instead of driving the dimer center of mass directly, as for charged adatoms and dimers, here we only force the overdamped internal coordinate η, which, in turn, couples to the substrate to produce a net dimer current [19].

III. CURRENT MAXIMIZATION

In the case when the dimer-substrate interaction is charge insensitive (i.e, not electrostatic [14]), the net current is finite even if the two dimer heads are set free, i.e., for $\alpha=0$. This happens because a time periodic drive rectifies the two dimer heads in the same direction, no matter what their charge. As a consequence, the time-averaged dimer current is nonzero, $\bar{J} \equiv \langle \dot{\mu} \rangle = \langle \dot{x} \rangle = \langle \dot{y} \rangle$, while the corresponding electric current, $Q\langle \dot{\eta} \rangle$, vanishes. On the contrary, for the charge-sensitive (i.e., mostly electrostatic) interaction in Eq. (1), opposite charges get rectified in opposite directions, thus suppressing the dimer current but not the electric current. In the limit of a very strong coupling, $\alpha \to \infty$, both the dimer and the electric current vanish, regardless of the dimer-substrate interaction, because the dimer behaves like a neutral rod, that is, decoupled from the external field $E(t)$. Thus, rectification occurs only due to the damped forced oscillations of the dimer; it vanishes when the internal variable η is either frozen, $\alpha \to \infty$, or dynamically irrelevant, $\alpha=0$.

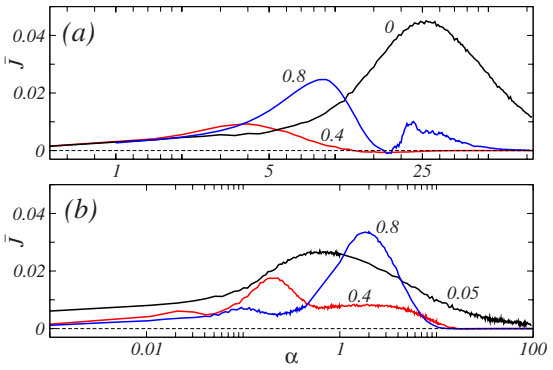

FIG. 2. (Color online) $\bar{J}$ vs. α for neutral dimers with different d (in the legends) and binding potentials: (a) W_2 of Eq. (2), and (b) W_4 of Eq. (3). The driving field is a sinusoidal waveform with $E=6$ and $\omega=6$. Other simulation parameters are: $Q=1$, $T=0.25$, and $U(x)$ as in Eq. (6) with $x_0=0.32$.

In the intermediate case of an elastic neutral dimer on a charge-sensitive substrate, we expect that the net dimer current attains a maximum for one or more finite values of the elastic constant α. To demonstrate this effect, we chose the asymmetric charged filament potential,

$$U(x) = \sin[2\pi(x+x_0)] + 0.25\cos(4\pi x), \qquad (6)$$

with $L=1$. Here the tunable phase constant x_0 was introduced to vary the potential symmetry. In particular, for $x_0=k/4$, $k=0,\pm 1,\pm 2,\ldots$, $U(x)$ is mirror symmetric. This implies that for $\alpha=0$, i.e., in the case of loose charged adatoms, the net current vanishes. On the other hand, for $x_0=\frac{1}{4}(k+\frac{1}{2})$, $U(x)$ coincides with the standard biharmonic ratchet potential investigated in the literature [16,20].

The time-averaged dimer current $\bar{J}$, obtained by numerically solving Eqs. (4) for a sinusoidal $E(t)$, is plotted in Fig. 2 as a function of α for both the quadratic, W_2, and the quartic binding potential, W_4. The optimal values of the elastic constant that maximize the current, strongly depends on the shape of the binding potential, $W(|x-y|)$, and the dimer rest length. For the connection between diffusion and internal dynamics of a dimer, the reader is referred to the earlier literature on the subject [3,9,10].

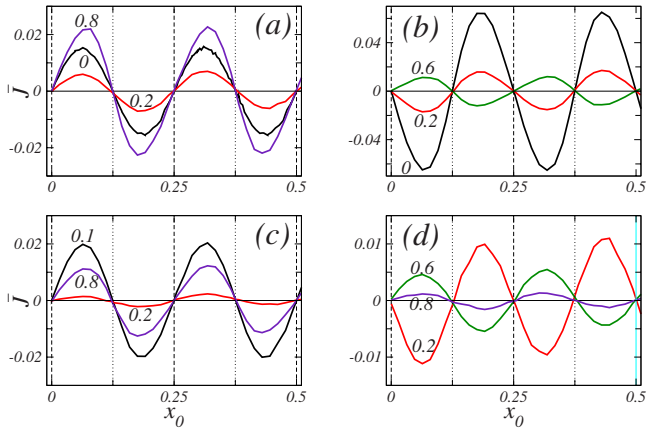

FIG. 3. (Color online) $\bar{J}$ vs. x_0 for different d (in the legends): (a) sine-wave drive, $W=W_2$, (b) square-wave drive, $W=W_4$, (c) sine-wave drive, $W=W_2$, (d) square-wave drive, $W=W_4$. Other simulation parameters are: $Q=1$, $T=0.25$, $E=6$, and $\omega=6$; the binding potentials W_2 and W_4 are, respectively, as in Eqs. (2) and (3), both with $\alpha=10$; the ratchet potential $U(x)$ is as in Eq. (6).

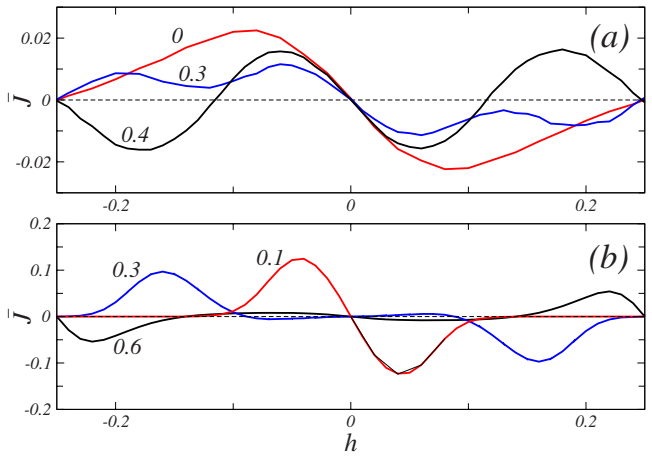

FIG. 4. (Color online) $\bar{J}$ vs h, for different d (in the legends) and an ac drive with square waveform. Here, h controls the asymmetry of the binding potential (see text), i.e., (a) $W(x)=W_2(x-h)$, (b) $W(x)=W_4(x-h)$. The remaining simulation parameters are as in Fig. 3.

IV. DIMER GLOBAL SYMMETRIES: CURRENT SUPPRESSION

As already pointed out, an ac driven charged adatom is rectified as long as its substrate is asymmetric with respect to mirror reflection [15]. The same condition applies to the rectification of a neutral dimer on a charge insensitive substrate [14]. Contrary to these two examples, we found that for the charge-sensitive substrate of Eq. (1), the dimer current vanishes as an effect of global dynamical symmetries of the system (4), even when the reflection symmetry of $U(x)$ is broken. Such symmetries can be explored by looking at the effective potential, $U_{\text{eff}}(\mu,\eta)$, and tuning the phase constant x_0 of $U(x)$. The situation considered here should be contrasted with that analyzed in Ref. [4], where $U(x)$ was kept mirror symmetric at all times, while a tunable dimer-drive coupling allowed to control the asymmetry of the system upon dimer head exchange.

For an unbiased time periodic drive $F(t)$, the net current $\bar{J}$ is nonzero only if the following two symmetries of U_{eff}, Eq. (5), are simultaneously broken: (A) symmetry with respect to the sign inversion of both coordinates μ and η, i.e., $U_{\text{eff}}(\mu,\eta)=U_{\text{eff}}(-\mu,-\eta)$, and (B) symmetry with respect to the sign inversion of μ, i.e., $U_{\text{eff}}(\mu,\eta)=U_{\text{eff}}(-\mu,\eta)$.

If the binding potential W is itself a symmetric function of η, symmetry A and B hold for $x_0=k/4$ and $x_0=\frac{1}{4}(k+\frac{1}{2})$, respectively, with $k=0,\pm1,\pm2,\ldots$. Most remarkably, the substrate potential $U(x)$ is asymmetric for $x_0=\frac{1}{4}(k+\frac{1}{2})$, but this does not suffice to warrant rectification for a neutral dimer.

If either dimer symmetry A or B is unbroken, the net current vanishes regardless of the shape of the binding potential or the dimer rest length. This result is illustrated in Fig. 3, where $\bar{J}$ is plotted against x_0 for different drive waveforms, binding potentials, and dimer lengths.

Symmetry A can also be broken by taking an asymmetric binding potential. This condition can be implemented, for instance, by introducing the shifted potential $W(x-h)$, which describes a polar dimer with two equally probable configurations, or opposite polarization states: a stretched state with rest length $d+h$ and a compressed state with rest length $d-h$. The dimer current $\bar{J}$ as a function of h is displayed in Fig. 4 for $x_0=1/4$, different dimer lengths, and both binding potentials, W_2 and W_4. No matter what the choice for W or d, the current vanishes at $h=\pm1/4$. This can be explained as follows. For $h=0$, $U_{\text{eff}}(\mu,\eta)$ exhibits symmetry A. Increasing (or decreasing) h breaks that symmetry, which gets restored only for $h=\pm1/4$, as apparent upon remarking that $U_{\text{eff}}(\mu,\eta)$ is invariant under the transformations $\eta\to\eta+h$ and $\mu\to\mu+h$.

V. ANALYTICAL RESULTS

The role of symmetry A and B in preventing dimer rectification can be regarded as an instance of the supersymmetry mechanism reviewed in Ref. [15], where the asymmetry of the substrate alone is not a sufficient condition to activate the ratchet mechanism.

A. Adiabatic square-wave drive

The suppression of the dimer current under symmetry A or B of the effective potential can be explained analytically for the study case of an adiabatically slow drive with square waveform. To compute the time-averaged dimer current we had recourse to the Fokker-Planck equation corresponding to the Langevin equations (4),

$$\frac{\partial P}{\partial t}=-\frac{\partial J_\mu}{\partial \mu}-\frac{\partial J_\eta}{\partial \eta}, \tag{7}$$

where the μ and η components of the instantaneous current densities $J_\mu(\mu,\eta)$ and $J_\eta(\mu,\eta)$ are, respectively,

$$J_\mu=-\left[\frac{\partial U_{\text{eff}}}{\partial \mu}+T\frac{\partial}{\partial \mu}\right]\frac{P}{2},$$

$$J_\eta = -\left[\frac{\partial U_{\rm eff}}{\partial \eta} + 2F(t) + T\frac{\partial}{\partial \eta}\right]\frac{P}{2}, \tag{8}$$

and the probability density $P(\mu,\eta,t)$ is normalized to one. This equation must be supplemented by natural boundary conditions in the η direction and periodic boundary conditions in the μ direction.

The instantaneous dimer current $J(t)$ is obtained by integrating the density J_μ over η and μ with appropriate boundary conditions, i.e.,

$$J(t) = \int_0^1 d\mu \int_{-\infty}^{+\infty} d\eta J_\mu(\mu,\eta,t), \tag{9}$$

so that

$$\bar{J} = \frac{\omega}{2\pi}\int_0^{2\pi/\omega} J(t)dt. \tag{10}$$

Note that for *constant* external fields $\pm E$, the Fokker-Planck equation (7) admits of stationary solutions

$$P_s^{(\pm)}(\mu,\eta) = \mathcal{N}\exp\left(-\frac{U_{\rm eff}(\mu,\eta) \mp 2QE\eta}{T}\right), \tag{11}$$

with normalization constant $\mathcal{N}$. Accordingly, the current densities J_μ and J_η are identically zero. This underlines the essential difference between ratcheting a charged adatom and a neutral dimer (on a periodic charge-sensitive or insensitive substrate, alike). In the former case, for a charged adatom (but even for a charged dimer) and adiabatically low frequencies of the square-wave oscillating field $E(t)$, the time-averaged current $\bar{J}$ can be approximated to $\bar{J} = \frac{1}{2}(J^{(+)} + J^{(-)})$, where $J^{(\pm)}$ are the corresponding stationary currents in the presence of the dc fields $\pm E$. As $J^{(+)} > 0$ and $J^{(-)} < 0$, with $|J^{(+)}| \neq |J^{(-)}|$, the adiabatic limit of $\bar{J}$ is frequency independent, i.e., $\bar{J}$ is finite, actually the largest, for $\omega \to 0$ (*rocked* ratchet [15]).

On the contrary, according to Eq. (11), for a neutral dimer the static currents $J^{(\pm)}$ vanish, no matter what the system parameters. A finite net current may only set on during the relatively short switch transients, when the sign of the square waveform $E(t)$ changes abruptly from positive to negative and vice versa, $\pm E \to \mp E$. During such transients, the instantaneous probability density, $P(\mu,\eta,t)$, switches back and forth between the two stationary densities $P_s^{(\pm)}(\mu,\eta)$ of Eq. (11). Clearly, the finite duration of the two switch transients does not depend on the drive period. Therefore, for $\omega \to 0$ the time-averaged dimer current $\bar{J}$ becomes proportional to ω (*pulsated* ratchet [15]), namely,

$$\bar{J} = \frac{\omega}{2\pi}\left(\int_0^{\tau_1} J^{(+-)}(t)dt + \int_0^{\tau_2} J^{(-+)}(t)dt\right), \tag{12}$$

where $\tau_1(\tau_2)$ is the transient time for the switches $+E \to -E(-E \to +E)$. The instantaneous currents $J^{(+-)}(t)$ and $J^{(-+)}(t)$ are then given by Eq. (9), respectively, with $E < 0$ and $E > 0$ and initial probability densities $P_s^{(\pm)}(\mu,\eta)$ (see also next section).

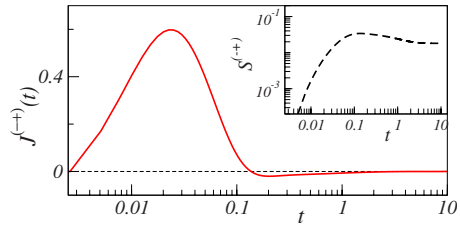

FIG. 5. (Color online) Instantaneous current $J^{(-+)}(t)$ during a switch, from −4 to +4, of the msquare wave oscillating field $E(t)$, as obtained numerically by integrating Eq. (7) with $x_0 = 1/4$ (symmetry A) and initial distribution $P_s^{(-)}$, Eq. (11). Other simulation parameters are: $Q=1$, $T=0.4$, and $\omega = 10^{-2}$; the binding potential W_2 is as in Eq. (2) with $d=0.4$ and $\alpha=10$; the ratchet potential $U(x)$ is as in Eq. (6). Inset: the corresponding accumulated current $S^{(-+)}(t) = \int_0^t J^{(-+)}(s)ds$.

B. Symmetries of the Fokker-Planck operator

Current suppression in the presence of symmetry A and B can now be explained by using Eq. (12).

(i) If $U_{\rm eff}$ is A-symmetric, within a drive cycle each transient current burst $\int_0^{\tau_1} J^{(+-)}(t)dt$ is exactly compensated by the opposite current burst, $\int_0^{\tau_2} J^{(-+)}(t)dt$.

(ii) If the effective potential $U_{\rm eff}$ is B-symmetric, then, the instantaneous currents $J^{(-+)}(t)$ and $J^{(+-)}(t)$ are exactly zero at any time.

Both circumstances (i) and (ii) imply identically zero net currents.

The rigorous proof of statements (i) and (ii) is as follows. Let us consider, first, the case of symmetry A in (i). Current bursts $\int_0^{\tau_1} J^{(+-)}(t)dt$ are obtained by solving the Fokker-Planck equation Eq. (7) with initial condition $P_s^{(+)}$, given in Eq. (11). The final state, after the $+E \to -E$ switch, is represented by the stationary solution of Eq. (7) with $E(t) = -E$, $P_s^{(-)}$. However, since the effective potential is symmetric under sign reversal of both coordinates, $U_{\rm eff}(-\mu,-\eta) = U_{\rm eff}(\mu,\eta)$, we conclude that the Fokker-Planck operator in Eq. (7) is antisymmetric with respect to the simultaneous transformations $\mu \to -\mu$, $\eta \to -\eta$, and $E \to -E$. As the dynamical symmetry of the time-dependent equation (7) can be restored by further imposing time reversal, $t \to -t$, it follows immediately that $\int_0^{\tau_1} J^{(+-)}(t)dt$ and $\int_0^{\tau_2} J^{(-+)}(t)dt$ must be opposite, i.e., their sum is identically zero.

The case of symmetry B is simpler. If $U_{\rm eff}$ is symmetric for $\mu \to -\mu$, it is clear that the Fokker-Planck operator in Eq. (7) is also symmetric for $\mu \to -\mu$. Therefore, regardless of the initial conditions, the instantaneous current $J(t)$ in Eq. (10) is identically zero at any time.

In Fig. 5, we plotted the instantaneous current $J^{(-+)}(t)$ after a $-E \to +E$ switch together with the corresponding accumulated current, $S^{(-+)}(t) = \int_0^t J^{(-+)}(s)ds$, for an A-symmetric dimer configuration with $x_0 = 1/4$. To this end we numerically integrated the time-dependent Fokker-Planck equation in Eq. (7) with the initial probability density $P_s^{(-)}$, Eq. (11), and symmetric binding potential W_2. We also checked that the current $J^{(+-)}(t)$ (not shown) is opposite to $J^{(-+)}(t)$, as expected. The time evolution of the density $P(\mu,\eta,t)$ is illustrated in Fig. 6 for the subsequent switch transient, $+E \to -E$.

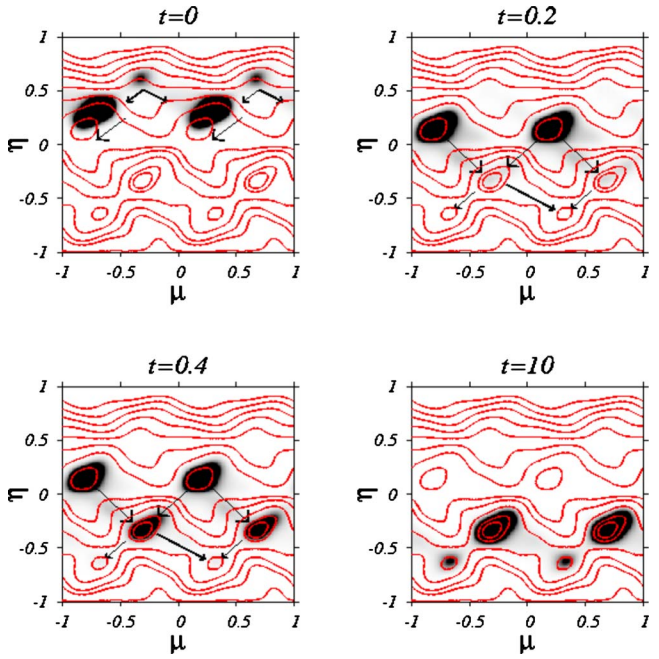

FIG. 6. (Color online) Different transient stages corresponding to a switch of the square-wave oscillating field $E(t)$, from +4 to −4. All remaining simulation parameters are as in Fig. 5 (symmetry A). The distribution densities are encoded by using different gray levels. Contour lines represent equipotential curves of the effective potential after switching, $U_{\text{eff}}(0)+8\eta$ (see text). Arrows indicate the probability flows in the two relaxation stages.

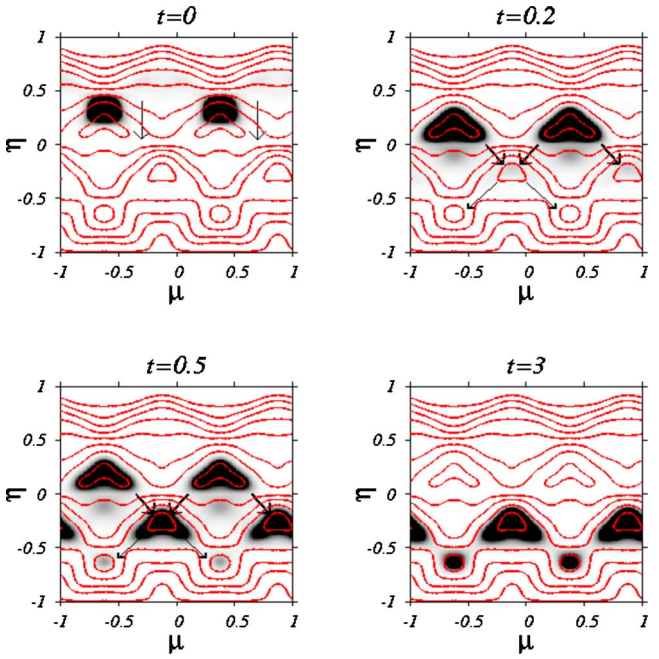

FIG. 7. (Color online) Different transient stages corresponding to a switch of the square-wave oscillating field $E(t)$, from +4 to −4, for a B-symmetric dimer dynamics. All simulation parameters and graphics codes are as in Fig. 6, but for $x_0=1/8$.

On comparing Figs. 5 and 6, it is apparent that each transient can be divided into two stages, a fast and a slow one. Let us consider for clarity the $+E\rightarrow -E$ switch depicted in Fig. 6. Initially, $t=0$, the periodic two-dimensional probability density, $P(\mu,\eta,t)$, is at equilibrium in the *tilted* effective potential, $U_{\text{eff}}-2QE\eta$. During the fast transient stage its maxima shift toward the nearest *local* minima of the new tilted effective potential, $U_{\text{eff}}+2QE\eta$. This produces a rather large negative current surge (like in Fig. 5, but with reversed sign!). The time duration of this stage is very short; it is over by $t=0.2$. During the subsequent slow stage, transitions occur form the local toward the *global* minima of $U_{\text{eff}}+2QE\eta$; accordingly, $P(\mu,\eta,t)$ relaxes toward the new stationary distribution $P_s^{(-)}$ and $J^{(+-)}(t)$ turns from negative to positive.

We estimated the time scale of the slow stage by using the two-dimensional Kramers' rate formula for the escape of a Brownian particle out a local minimum, over a saddle point [21]. At low temperatures, the rate constant is given by

$$r=\frac{1}{2\pi}\sqrt{-\lambda_1\lambda_2\frac{\lambda_s}{\lambda_u}}\exp\left(-\frac{\Delta U}{T}\right), \tag{13}$$

where ΔU is the barrier height, λ_1 and λ_2 are the two stable (positive) eigenvalues at a local minimum of the new potential $U_{\text{eff}}+2QE\eta$, and λ_s and λ_u are respectively, the stable (positive) and unstable (negative) eigenvalues at the saddle (escape) point.

In Fig. 6, the density $P(\mu,\eta,t)$ at $t=0.2$ is almost entirely concentrated around its local minima with positive η, one per spatial unit cell, L. There are two distinct escape paths connecting each such local minimum to the two global minima nearest to it, also one per unit cell, but with negative η. In Fig. 6, the direction of these transitions are indicated by arrows. We checked that the Kramers' rates associated with these two escape paths control sign and magnitude of the slowly decaying $J^{(\pm\mp)}(t)$ tail, see Fig. 5.

For the sake of a comparison, the time evolution of a B-symmetric density $P(\mu,\eta,t)$ is displayed in Fig. 7. In this geometry, both the fast and the slow stage correspond to zero currents in the μ direction. Note that our conclusion holds even if, for the case considered in Fig. 7, $U(x)$ coincides with the reference biharmonic ratchet potential introduced in Ref. [16].

VI. CONCLUSION

We now summarize our results. We considered a neutral dimer diffusing along an electrically charged filament in one dimension, with spatially periodic charge distribution. In our model, the interaction between the dimer and the filament was assumed to be charge-sensitive, meaning that opposite charges get rectified to opposite directions when set free.

Unlike a single charged adatom or a neutral dimer with charge insensitive interaction, the net dimer current in the presence of charge-sensitive interaction is shown to depend on the global dynamical symmetries of the system. In fact, the dimer current can vanish even for asymmetric filament potentials.

Therefore, we characterized the system in terms of an effective two-dimensional potential, $U_{\mathrm{eff}}(\mu,\eta)$, which depends on the coordinate of the dimer center of mass, μ, and its instantaneous half-length η. For an unbiased external drive, the dimer current is nonzero only if the following symmetries of U_{eff} are simultaneously broken: (A) symmetry under coordinate sign reversal, $\mu\rightarrow-\mu$ and $\eta\rightarrow-\eta$, and (B) symmetry under μ sign reversal, $\mu\rightarrow-\mu$. These findings were demonstrated numerically for two different dimer binding potentials and two different drive waveforms. A simple analytical argument confirms that dimer rectification sets on, indeed, only when both symmetries are broken.

Moreover, we showed that, no matter what the choice of the binding potential, the net dimer current can be maximized by tuning the dimer elastic constant. In the opposite limits of loose dimer heads (zero elastic constant) or rigid dimer (infinite elastic constant), the dimer net current is identically zero.

ACKNOWLEDGMENTS

One of us (A.P.) would like to thank M. Bestehorn for granting him access to the computer cluster, where most of the simulations were carried out. This work was partly supported by the EPSRC U.K. (Grants No. Ep/F005482/1 and No. Ep/D072581/1).

[1] T. E. Dialynas and G. P. Tsironis, Phys. Lett. A **218**, 292 (1996).
[2] R. Tsekov and E. Ruckenstein, Surf. Sci. **344**, 175 (1995).
[3] O. M. Braun, Phys. Rev. E **63**, 011102 (2000).
[4] S. Cilla, F. Falo, and L. M. Floría, Phys. Rev. E **63**, 031110 (2001).
[5] J. L. Mateos, Physica D **168**, 205 (2002).
[6] C. Fusco and A. Fasolino, Thin Solid Films **428**, 34 (2003).
[7] A. H. Romero, A. M. Lacasta, and J. M. Sancho, Phys. Rev. E **69**, 051105 (2004).
[8] J. L. Mateos, Physica A **351**, 79 (2005).
[9] J. Menche and L. Schimansky-Geier, Phys. Lett. A **359**, 90 (2006).
[10] E. Heinsalu, M. Patriarca, and F. Marchesoni, Phys. Rev. E **77**, 021129 (2008).
[11] J. Bammert, S. Schreiber, and W. Zimmermann, Phys. Rev. E **77**, 042102 (2008).
[12] S. von Gehlen, M. Evstigneev, and P. Reimann, Phys. Rev. E **77**, 031136 (2008).
[13] S. von Gehlen, M. Evstigneev, and P. Reimann, Phys. Rev. E **79**, 031114 (2009).
[14] A. Pototsky, N. B. Janson, F. Marchesoni, and S. Savel'ev, EPL **88**, 30003 (2009).
[15] P. Reimann, Phys. Rep. **361**, 57 (2002).
[16] R. Bartussek, P. Hänggi, and J. G. Kissner, Europhys. Lett. **28**, 459 (1994).
[17] M. O. Magnasco, Phys. Rev. Lett. **71**, 1477 (1993).
[18] J. Howard, *Mechanics of Motor Proteins and the Cytoskeleton* (Sinauer, Sunderland, MA, 2001).
[19] S. Savel'ev, F. Marchesoni, and F. Nori, Phys. Rev. Lett. **91**, 010601 (2003).
[20] P. Hänggi and F. Marchesoni, Rev. Mod. Phys. **81**, 387 (2009).
[21] C. Gardiner, *Handbook of Stochastic Methods* (Springer, Berlin, 1996).